Immunity
Article

The Dendritic Cell Receptor Clec9A Binds Damaged Cells via Exposed Actin Filaments

Jian-Guo Zhang,[1,2,13] Peter E. Czabotar,[1,2,13] Antonia N. Policheni,[1,2] Irina Caminschi,[1,2,5] Soo San Wan,[1] Susie Kitsoulis,[1,5] Kirsteen M. Tullett,[1,5] Adeline Y. Robin,[1,2] Rajini Brammananth,[6] Mark F. van Delft,[8,9] Jinhua Lu,[10] Lorraine A. O'Reilly,[1,2] Emma C. Josefsson,[1,2] Benjamin T. Kile,[1,2] Wei Jin Chin,[1,3] Justine D. Mintern,[1,4] Maya A. Olshina,[1,2] Wilson Wong,[1] Jake Baum,[1,2] Mark D. Wright,[11] David C.S. Huang,[1,2] Narla Mohandas,[12] Ross L. Coppel,[6,7] Peter M. Colman,[1,2] Nicos A. Nicola,[1,2] Ken Shortman,[1,2,*] and Mireille H. Lahoud[1,2,5,*]
[1]The Walter and Eliza Hall Institute of Medical Research, Parkville, Victoria 3052, Australia
[2]Department of Medical Biology
[3]Department of Microbiology and Immunology
[4]Department of Biochemistry and Molecular Biology
The University of Melbourne, Parkville, Victoria 3010, Australia
[5]Centre for Immunology, Burnet Institute, Melbourne, Victoria 3004, Australia
[6]Department of Microbiology
[7]Faculty of Medicine
Monash University, Clayton, Victoria 3800, Australia
[8]Division of Stem Cell and Developmental Biology, Campbell Family Institute for Cancer Research/Ontario Cancer Institute, Toronto, ON M5G 1L7, Canada
[9]Toronto General Research Institute, University Health Network, Toronto, ON M5G 1L7, Canada
[10]Yong Loo Lin School of Medicine, National University of Singapore, Blk MD4, 5 Science Drive 2, Singapore 117597, Singapore
[11]Department of Immunology, Monash University, Melbourne, Victoria 3004, Australia
[12]Red Cell Physiology Laboratory, New York Blood Center, New York, NY 10065, USA
[13]These authors contributed equally to this work
*Correspondence: shortman@wehi.edu.au (K.S.), lahoud@burnet.edu.au (M.H.L.)
DOI 10.1016/j.immuni.2012.03.009

SUMMARY

The immune system must distinguish viable cells from cells damaged by physical and infective processes. The damaged cell-recognition molecule Clec9A is expressed on the surface of the mouse and human dendritic cell subsets specialized for the uptake and processing of material from dead cells. Clec9A recognizes a conserved component within nucleated and nonnucleated cells, exposed when cell membranes are damaged. We have identified this Clec9A ligand as a filamentous form of actin in association with particular actin-binding domains of cytoskeletal proteins. We have determined the crystal structure of the human CLEC9A C-type lectin domain and propose a functional dimeric structure with conserved tryptophans in the ligand recognition site. Mutation of these residues ablated CLEC9A binding to damaged cells and to the isolated ligand complexes. We propose that Clec9A provides targeted recruitment of the adaptive immune system during infection and can also be utilized to enhance immune responses generated by vaccines.

INTRODUCTION

Dendritic cells (DCs) are an essential link between the adaptive and innate immune systems. DCs initiate adaptive immune responses by processing and presenting antigens to T cells (Banchereau et al., 2000; Steinman et al., 2003). DCs also monitor the environment by using a series of innate receptors for pathogen-associated molecular patterns (PAMPs) and damaged cell-associated molecular patterns (DAMPs). This enables DCs to adjust the balance between tolerance and immunity and to tailor the immune response to particular pathogens. Particular DC subsets are specialized in detailed aspects of these general functions. In the mouse, the $CD8^+$ DCs are especially efficient at the uptake and processing of material from dead cells (Shortman and Heath, 2010). Human $CD141^+$ ($BDCA\text{-}3^+$) DCs have been identified as the lineage and functional equivalents of the mouse $CD8^+$ DCs (Villadangos and Shortman, 2010), and therefore they would be expected to have a particular pattern of PAMP and DAMP receptors related to these functions.

One such DAMP receptor on mouse $CD8^+$ DCs and on human $CD141^+$ DCs is Clec9A (also called DNGR-1) (Caminschi et al., 2008; Huysamen et al., 2008; Sancho et al., 2008); our laboratory and that of Reis e Sousa (Sancho et al., 2009) have found that it binds to dead cells. Clec9A also regulates the cross-presentation of dead cell-associated antigens in a Syk-dependent manner (Sancho et al., 2009). There is particular interest in Clec9A because it has been found to be an especially effective target for delivery of antigens to DCs, and therefore promotes immune responses (Caminschi et al., 2008; Idoyaga et al., 2011; Lahoud et al., 2011; Sancho et al., 2008). Thus, Clec9A has great promise for enhancing vaccine efficacy.

Here we have sought to understand the function of Clec9A as a DAMP receptor. We have presented the crystal structure of the Clec9A C-type lectin-like domain (CTLD) and identified a region involved in ligand recognition. We have shown that the ligand is

a cytoskeletal component of nucleated and nonnucleated cells, exposed upon cell death and membrane rupture as would occur after cellular lysis by pathogens or physical damage. We have identified the ligand as a filamentous form of actin normally complexed to the calponin homology-based actin binding domain (ABD) motif of cytoskeletal molecules, including spectrin β and α-actinin.

RESULTS

Mouse and Human Clec9A Bind to Damaged Cells

As reagents to identify Clec9A ligands, we generated recombinant tagged soluble forms of the ectodomains of mouse Clec9A (mClec9A) and human CLEC9A (hCLEC9A). These consist of a FLAG-tag, a biotinylation consensus sequence, and either the full ectodomain (Clec9A-ecto), the Clec9A-CTLD, or the Clec9A-stalk (Figures S1A–S1C available online). To determine whether Clec9A recognizes self-components, a range of mouse and human cells were stained with the Clec9A ectodomains. No binding was observed to the surface of viable cells, but binding was observed to dead cells identified by propidium iodide (PI) staining, as previously described (Sancho et al., 2009). We then investigated various stages of cell death, by following thymocytes undergoing apoptosis induced by γ-irradiation or mouse embryonic fibroblasts (MEFs) undergoing apoptosis induced by BH3-only ligands (van Delft et al., 2006). We stained cells with Annexin V, an early marker of apoptosis, and with PI, a late marker that stains nuclei once the cell membrane is damaged. mClec9A-ecto strongly bound to late-stage apoptotic, secondary necrotic cells (Annexin V^+PI^+) but not to early-stage apoptotic cells where cell membranes are still intact (Annexin V^+PI^-) (Figure S1D). Both mClec9A and hCLEC9A strongly bound to the late-stage apoptotic MEFs, but not to live cells (Figure S1E). In all cases binding to dead cells was much higher than any ''nonspecific'' binding seen with other C-type lectins tested, namely Cire (Figures 1A–1D and S1D–S1I) and Clec12A.

To determine whether membrane rupture was sufficient to reveal the ligand, cells were stained immediately after freezing and thawing. This served as a model of primary necrosis. mClec9A and hCLEC9A ectodomains bound strongly to freeze-thawed mouse 3T3 cells (Figure S1F) or human 293 cells (Figure S1G), as well as to fixed and permeabilized cells (data not shown). Sancho et al. (2009) have drawn similar conclusions.

The binding of mClec9A or hCLEC9A to dead cells occurred in the presence of ethylenediamine tetraacetic acid (EDTA) (Figure S1G). Thus, ligand recognition was not dependent on readily chelated divalent metal ions, as would be expected of a classical C-type lectin binding to a carbohydrate. Treatment of late-stage apoptotic cells with proteases, but not with nucleases, reduced the Clec9A binding, suggesting that the ligand was protein (Figure S1H). However, pretreatment of viable cells with trypsin prior to freeze thawing did not eliminate Clec9A binding after freeze thawing, emphasizing that the ligand was intracellular and revealed only on membrane disruption.

Cell and Species Distribution of the Clec9A Ligand

Both mClec9A and hCLEC9A ectodomains bound to all dead mouse or human nucleated cells tested, including cultured cell lines and primary cells (Figures 1 and S1). They also bound to freeze-thawed Chinese hamster (CHO), African green monkey (Vero) (data not shown), and freeze-thawed insect (SF21) cells, but not to freeze-thawed bacteria or yeast (Figure 1A). Thus, recognition of the dead cell ligand was conserved across a wide evolutionary range. A clue to the nature of the ligand was the finding that mClec9A-ecto and hCLEC9A-ecto also bound to disrupted nonnucleated cells, including apoptotic mouse platelets (Figure 1B) and mouse and human erythrocyte (RBC) ghosts prepared by saponin treatment (Figures 1C and S1I).

The binding of the Clec9A CTLD or the Clec9A stalk was compared to the binding of the full ectodomain. At saturating concentrations, both mClec9A-CTLD and hCLEC9A-CTLD showed similar binding to both dead cells and saponin-lysed erythrocytes as the full ectodomains (Figure 1C). In contrast, the Clec9A stalk region showed no binding.

Examination of mClec9A-ecto binding to permeabilized 3T3 cells by immunofluorescence microscopy revealed staining over the cytoplasmic area, in a pattern indicative of membrane or cytosolic localization (Figure 1D). Colocalization studies with the cytoskeletal protein actin were performed with an actin antibody that labels all cellular actin and with phalloidin which labels filaments of actin (F-actin). This revealed that Clec9A binding localized with actin filaments but not with all of the cellular actin (Figures 1E and 1F). This directed attention to cytoskeletal complexes associated with actin filaments.

Clec9A Binds to Cytoskeletal Components Including Complexes Containing Spectrin

Several approaches suggested that the intracellular ligand for Clec9A could be a cytoskeletal component. Mass spectrometry analysis of Clec9A complexes isolated by coimmunoprecipitation from the lysates of mouse thymocytes and of a suspension-adapted subline of human embryonic kidney cells (Freestyle 293F) revealed a complex of cytoskeletal proteins that migrated at 250–300 kDa, including spectrin, filamin, myosin (Table S1), and smaller proteins including actin and actin-related proteins. However, the extraction of these poorly soluble complexes was inefficient and identification of a single protein ligand was challenging.

Selective extraction of spectrin from erythrocyte ghosts resulted in a marked reduction of binding of mClec9A-ecto to the ghosts (Figure 2A), suggesting that spectrin was a likely Clec9A ligand. Erythroid spectrin is composed of an αI (246 kDa) βI (280 kDa) heterodimer that self-associates to form a tetramer and binds to cytoskeletal proteins including actin and band 4.1 to form the membrane skeleton (An et al., 2011; Baines, 2010). We therefore tested the binding of mClec9A-ecto to a commercial preparation of human erythrocytic spectrin, by ELISA (Figure 2B). Analysis of this spectrin preparation by SDS-PAGE and protein staining (Figure S2A) indicated that the preparation was relatively pure as judged by the expected 246 kDa and 280 kDa sized protein bands, but minor bands were also evident. Mass spectroscopic analysis revealed a majority of peptides corresponding to the expected spectrin αI and spectrin βI, but also peptides corresponding to spectrin-associated proteins including actin, band 4.1, adducins, and tropomodulins (Table S2). High-affinity binding was observed to this commercial preparation of spectrin and associated proteins, compared to very

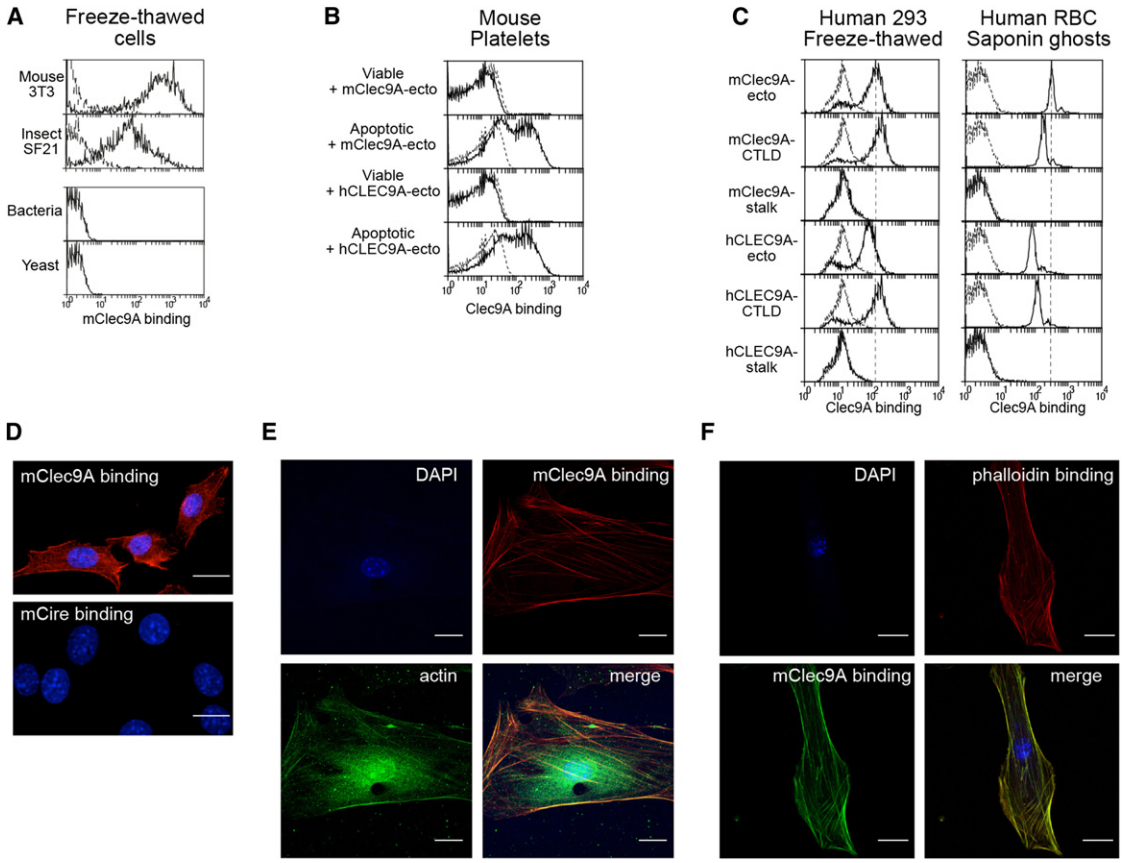

Figure 1. Clec9A Binds to Species-Conserved Components of Dead Cells

(A) Mouse 3T3 cells, insect SF21 cells, bacterial JM109 cells, and yeast (*Pichia pastoris*) cells were freeze-thawed twice then incubated with biotinylated mClec9A-ecto (solid line) or biotinylated control (Cire-ecto, dashed line). Binding was detected via SA-PE and flow cytometry.

(B) Mouse platelets were induced to undergo apoptosis by treatment with 0.5 μM ABT-737 for 90 min at 37°C. Control (viable) and ABT-737-treated (apoptotic) platelets were harvested and incubated with mClec9A-ecto (solid line), hCLEC9A-ecto (solid line), or Cire-ecto (background control, dashed line). Binding was detected via FITC-conjugated FLAG mAb and flow cytometry. Control platelets were confirmed to be Annexin V^- and ABT-737-treated platelets Annexin V^+.

(C) Human 293F cells were freeze-thawed. Human red blood cells (RBC) were isolated, permeabilized with PBS containing 0.15% saponin and 1× EDTA-free complete protease inhibitors (Roche), and repeatedly washed with the saponin-containing buffer in order to generate saponin-permeabilized RBC ghosts. Freeze-thawed human 293F cells and human RBC saponin-permeabilized ghosts were incubated with mClec9A and hCLEC9A-ectodomains (-ecto), C-type lectin like domains (-CTLD) or stalk regions (-stalk) (solid line), or Cire-ecto (dashed line). Binding was detected with a FITC-conjugated FLAG mAb and flow cytometry.

(D) Fixed and permeabilized mouse 3T3 cells were incubated with biotinylated mClec9A-ecto or Cire-ecto and binding detected with SA-Alexa594. Fibroblasts were counterstained with DAPI and analyzed by confocal microscopy. Scale bars represent 20 μM.

(E) Fixed and permeabilized mouse embryonic fibroblasts were incubated with biotinylated mClec9A-ecto or Cire-ecto and binding detected via SA-Alexa594. Cells were counterstained with DAPI and with a rabbit anti-actin Ab and binding detected with anti-rabbit Ig-Alexa488, then analyzed by confocal microscopy. Scale bars represent 20 μM.

(F) Fixed and permeabilized mouse embryonic fibroblasts were incubated with biotinylated mClec9A-ecto and binding detected via SA-Alexa488. Cells were counterstained with DAPI and with phalloidin-Alexa594, then analyzed by confocal microscopy. Scale bars represent 20 μM.

See also Figure S1 and Table S1.

low binding of the controls mCire-ecto and mClec12A-ecto. The mClec9A-ecto showed little binding to a commercial preparation of actin, because actin was considered a possible contaminant.

Clec9A Binds to a Higher-Order Complex Including Erythrocyte Spectrin

These results prompted an examination of the conditions required to extract spectrin as the putative Clec9A-binding ligand. Spectrin extractions from mouse erythrocyte ghosts prepared by osmotic lysis were performed at 4°C, which enables the extraction of spectrin in the form of tetramers and higher-order complexes, or at 37°C, which produces mainly spectrin dimers (Gratzer, 1982; Ungewickell and Gratzer, 1978). The isolated spectrin was coated onto ELISA plates and investigated for Clec9A binding. Binding of mClec9A-ecto was obtained to spectrin if isolated at 4°C, but not if isolated at 37°C (Figure 3A). The spectrin preparations were examined by SDS-PAGE (Figure 3B) and by mass spectrometry (Table S3). There were no differences detected between the two extracts, the major components being spectrin αI and spectrin βI together with actin and band 4.1.

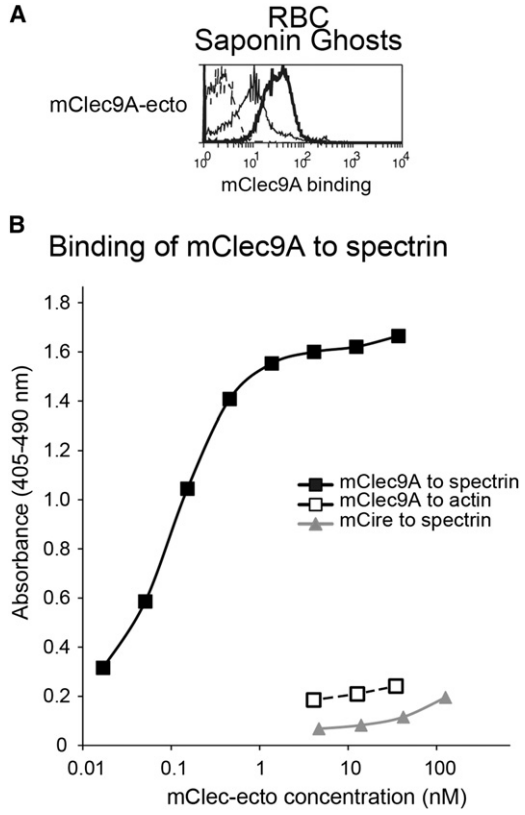

Figure 2. Mouse Clec9A Ectodomain Binds to Erythrocytic Spectrin

(A) Mouse saponin-permeabilized RBC ghosts were generated as in Figure 1C, then treated in the presence or absence of spectrin extraction buffer for 1 hr at 37°C. RBC ghost membranes were recovered by ultracentrifugation (26,000 × g, 40 min). Biotinylated mClec9A-ecto binding to untreated saponin ghosts (solid thick line), mClec9A-ecto binding to spectrin-extracted saponin ghosts (solid thin line), and Cire-ecto binding (dashed line) were detected via SA-PE and flow cytometry.

(B) Human erythrocytic spectrin (Sigma) and bovine muscle actin (Sigma) were coated onto ELISA plates and binding of mClec9A-ecto and mCire-ecto detected via anti-FLAG-HRP.

See also Figure S2 and Table S2.

This suggested that the differences in Clec9A binding were due to differences in the incidence of higher-order complexes. Accordingly, the two spectrin samples were analyzed by size-exclusion chromatography. Mouse erythrocyte spectrin gave one major peak of protein when isolated at 4°C (peak 1, Figure 3C), whereas isolation at 37°C yielded two peaks, a minor peak corresponding to peak 1 and a major peak 2 of smaller molecular size (Figure 3C). Fractions spanning these regions were coated onto ELISA plates and tested for their ability to bind mClec9A-ecto. The higher molecular size samples from peak 1 bound Clec9A, whereas material from peak 2 did not bind (Figure 3D). Analysis by SDS-PAGE revealed that although both peak 1 and peak 2 were primarily composed of spectrin, peak 1 contained two additional bands at 75 and 45 kDa, corresponding to band 4.1 and actin, respectively (Figure 3E). The commercial preparation of human erythrocyte spectrin also displayed a principle peak of protein eluting at the position of peak 1, and this retained all the ability to bind mClec9A-ecto (Figures S2B–S2D). Overall these experiments indicated that Clec9A binds to a complex of spectrin with associated proteins, but not to spectrin alone.

Clec9A Binds to a Higher-Order Complex Including Nucleated Cell Spectrin

Spectrin complexes are found in both erythrocytic and nonerythrocytic cells, although different subunits of spectrin are expressed in different cell types (Baines, 2010; Rotter et al., 2004; Uribe and Jay, 2009). To determine whether a spectrin complex represented a Clec9A ligand within nucleated cells, we isolated and analyzed by size-exclusion chromatography spectrin from 293F cells. A protein peak appeared in the same elution position as erythrocyte spectrin peak 1 (Figure 3F), separated from a spread of proteins of lower molecular sizes. When the fractions were coated on ELISA plates, mClec9A-ecto bound predominantly to fractions corresponding to peak 1 (Figure 3G). SDS-PAGE and mass spectroscopic analysis revealed that the major constituent of peak 1 from these nucleated cells was spectrin α and β chains, together with other protein components including actin (Figures 3H and 3I; Table S3). Thus Clec9A binds to a spectrin complex from nucleated as well as nonnucleated cells. Furthermore, a spectrin complex isolated from apoptotic cells was similarly bound by Clec9A (Figures S2E–S2G). Thus Clec9A recognition of spectrin complexes is maintained, even after apoptotic cell death and associated proteolysis. Importantly, the binding of mClec9A to spectrin complexes was stable over the pH range 7.4 to 4.0 (Figure S2H), indicating that Clec9A recognition of such complexes is likely to be stable in endosomal compartments of the cell.

Spectrin-Actin Interaction Required for Clec9A Binding

We sought to determine what features of the erythrocytic spectrin complexes were essential for recognition by Clec9A. Spectrin complexes were extracted from mouse erythrocyte ghosts at 4°C, then treated for 1 hr at 37°C to dissociate the complex into its individual components. Size-exclusion chromatography revealed that most of the complex had been dissociated, shifting to the lower molecular size peak 2 (Figure S3A). Binding of mClec9A-ecto to the dissociated spectrin preparation was greatly reduced and size-exclusion chromatography showed that the residual binding was restricted to the remaining undissociated complex in peak 1 (Figure S3B). Importantly, the dissociated spectrin at peak 2, now free of most other proteins (Figure S3C), showed no binding of Clec9A (Figure S3B). No binding was observed to fractions containing other dissociated protein components of the complex, nor was there binding under these conditions to the G-form of actin alone. The purified, dissociated, and nonbinding spectrin fractions of peak 2 were then concentrated and allowed to reassociate in the presence of either bovine muscle actin or bovine serum albumin (BSA) as a control for 2 hr at 30°C. Both samples showed partial reassociation, as judged by regeneration of the larger molecular size peak 1 on size-exclusion chromatography (Figure S3D). However, only the peak 1 complex reconstituted with actin showed pronounced binding to mClec9A-ecto (Figure S3E). Even the slight binding of the complex reconstituted with BSA could be attributed to traces of actin remaining in the preparation (Figures S3D and S3F). This indicated that Clec9A

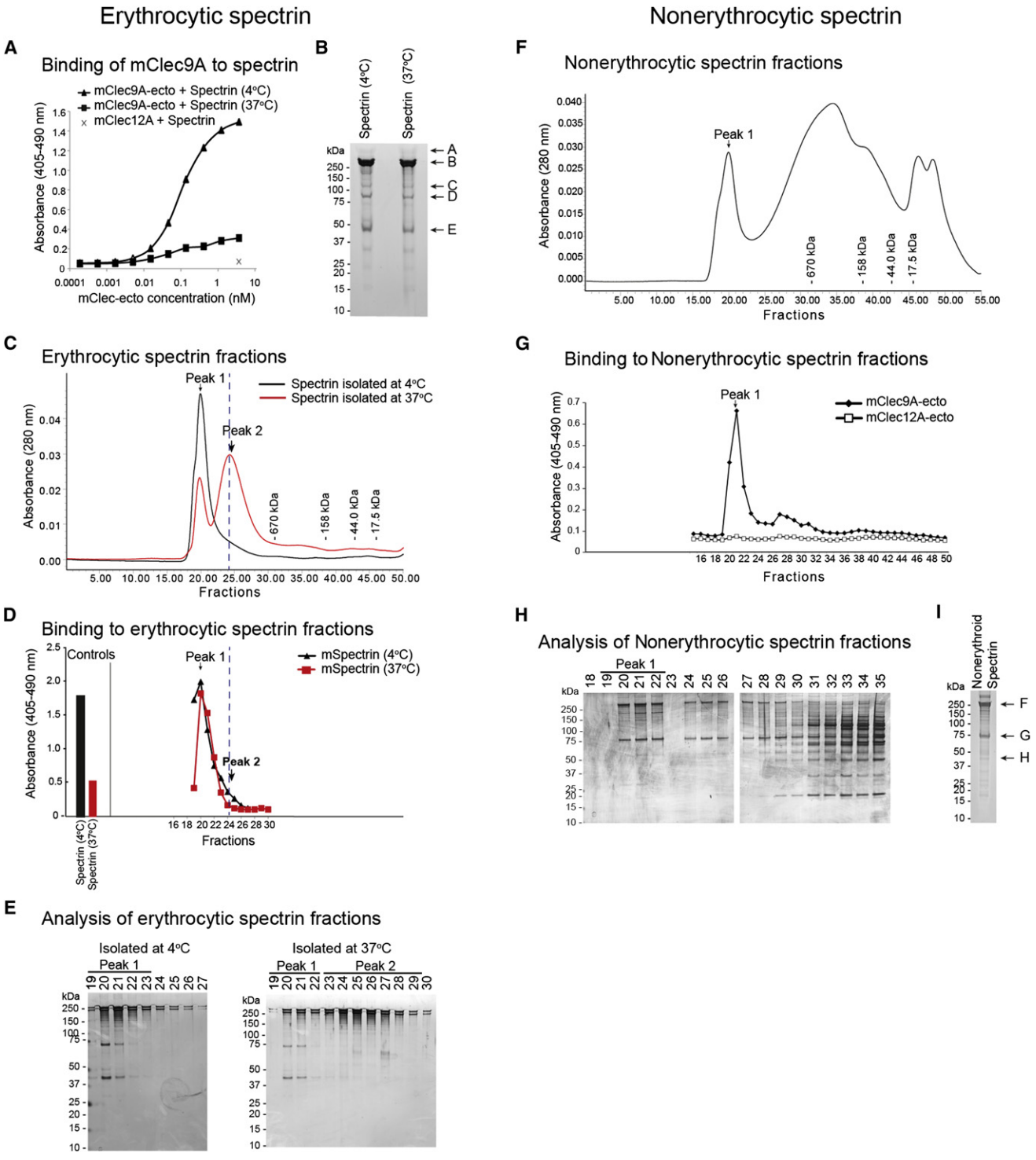

Figure 3. Mouse Clec9A Ectodomain Binds to Erythrocytic and Nonerythrocytic Spectrin Cytoskeletal Complexes

(A) Analysis of mouse Clec9A binding to spectrin by ELISA. Mouse erythrocytic spectrin, isolated at 4°C or at 37°C, was coated onto ELISA plates, and binding of mClec9A-ecto and the control, Clec12A-ecto, to erythrocytic spectrin was detected with anti-FLAG-HRP.

(B) Mouse erythrocytic spectrin (5 μg), isolated at 4°C or at 37°C, was analyzed by SDS-PAGE under reducing conditions. Protein bands were visualized, and bands A to E subjected to mass spectrometry analysis. See also Table S3.

(C) Analysis by size-exclusion chromatography (SEC) of mouse spectrin isolated from red blood cells at 4°C (black line) or 37°C (red line). Mouse erythrocytic spectrin was chromatographed on a Superose 6 column and fractions collected for subsequent analysis.

(D) mClec9A binding to SEC fractions of erythrocytic spectrin. Spectrin fractions (C) were coated onto ELISA plates, and binding of mClec9A-ecto (0.3 μg/ml) detected.

binds to a higher-order complex consisting of both spectrin and actin.

Minimal Requirements for a Spectrin-Actin Complex that Binds Clec9A

We then asked what regions of erythrocyte spectrin were essential for assembly of a Clec9A binding complex. Erythroid and nonerythroid spectrins contain multiple spectrin repeat elements, an actin binding domain (ABD) in the N terminus of β-spectrin, and a calmodulin-like domain at the C terminus of the α-spectrin (An et al., 2011; Baines, 2010). We therefore tested recombinant fragments of human erythrocytic spectrin (Figure 4A) for ability to bind mClec9A-ecto in the presence or absence of bovine muscle actin (Figure S4A). None of the individual fragments of spectrin showed binding, nor did actin alone. However, the complex of actin with the N-terminal domains of the β chain of spectrin (βI N-4), which encompasses the spectrin β1 actin-binding domain (ABD) and repeats 1–4, showed significant binding. We then compared the binding of Clec9A to a complex of muscle actin with either the N-terminal domains of spectrin βI (βI N-4) or with the ABD only (βI N). We found Clec9A binding activity was directed to the complex of spectrin βI ABD with actin (Figure 4B).

The binding of Clec9A to this reconstructed complex was lower than the binding to the commercial human erythrocyte spectrin sample, so we compared the effects of different forms of actin on Clec9A binding. There are three classes of actin: α-actins found in muscle and β- and γ-actins found in most cell types associated with the cytoskeleton (Bergeron et al., 2010). Therefore, we compared Clec9A binding to complexes of the spectrin βI ABD with muscle actin or with platelet actin (85% β-actin, 15% γ-actin). Clec9A binding to spectrin βI ABD with platelet actin was higher and comparable to that of commercial human erythrocytic spectrin (Figure 4B), indicating that the main determinant of Clec9A binding to erythrocytic spectrin is a complex of the spectrin βI ABD with cytoskeletal actins.

To test whether this binding of Clec9A to the spectrin-actin complex was related to the recognition of dead cells, Clec9A-ecto was preincubated with spectrin βI ABD and actin. This inhibited the ability of Clec9A-ecto to bind to dead cells, both freeze-thawed and apoptotic cells (Figure 4C), supporting the concept that Clec9A recognizes spectrin βI ABD-actin complexes by using similar determinants to the recognition of dead cells.

Other Actin-Complexed Cytoskeletal Proteins Bind Clec9A

The ABD of spectrin β chains is composed of two calponin homology domains of approximately 110 residues each. This domain is also found in other proteins of the spectrin family and several other actin binding proteins, including α-actinin, dystrophin, and filamin (Uribe and Jay, 2009; Korenbaum and Rivero, 2002). Accordingly, we compared the binding of Clec9A to a complex of the ABD of erythrocytic spectrin (spectrin βI N), nonerythrocytic spectrin (spectrin βII N), and human α-actinin 1 (α-actinin 1 N) in the presence and absence of platelet actin. The mClec9A-ecto showed significant and comparable binding to the complex of the ABD of erythrocytic and nonerythrocytic spectrins and α-actinin with platelet actin (Figures 4D and 4E) but not to the individual components of these complexes. Furthermore, preincubation of Clec9A with actin complexed with the ABD of erythrocytic spectrin, nonerythrocytic spectrin, and α-actinin 1 inhibited the ability of Clec9A-ecto to bind to dead cells (Figure S4B). In contrast, Clec9A did not bind actin complexed with an unrelated actin binding protein, Cofilin-1 (Figure S4C). Thus Clec9A recognizes a widespread form of actin complexed with ABDs with the 2 calponin homology domain motif. Importantly, Clec9A expressed in its native state on the surface of transfected CHO-K1 cells showed binding to actin complexed with the ABD of nonerythrocytic spectrin (Figure 4F).

Clec9A Recognizes F-Actin

From the preceding results, Clec9A might recognize a pattern formed by the complex between actin and the ABDs or a conformational form of actin induced by the interaction with ABDs. Focus shifted to actin itself when two of seven commercial preparations of actin showed direct binding to Clec9A in ELISA assays after preincubation at room temperature, in contrast to the results in Figures 4 and S4. To examine this further, the preparations were first incubated under conditions promoting the G-actin form, and then the G-actin was purified by size-exclusion chromatography to eliminate contaminating actin-binding proteins. G-actin was then converted to F-actin, incubated with mClec9A-ecto or Clec12A-ecto as control, and then centrifuged. Clec9A was found to sediment with F-actin to a much greater extent than Clec12A, showing that it had a capacity to recognize and bind to the filamentous conformation of actin itself (Figures 5A and 5B). We therefore propose that the role of the ABDs in Clec9A recognition is to promote or maintain the conformation of actin found in actin filaments.

Structure of the Clec9A C-Type Lectin-like Domain

We determined the crystal structure of the CTLD and compared it to other C-type lectin receptors. The CTLD of human CLEC9A (hCLEC9A) was expressed in 293F cells with an N-terminal FLAG tag. Glycosylation was eliminated through mutation of the sole glycosylation site (223-NCS-225) to the equivalent

(E) Analysis of erythrocytic spectrin fractions by SDS-PAGE. Erythrocytic spectrin fractions from SEC (C) were analyzed by SDS-PAGE under reducing conditions and protein bands visualized by silver staining.
(F) Analysis of human nonerythrocytic spectrin extract isolated from 293F cells at 4°C by SEC on a Superose 6 column.
(G) mClec9A binding to SEC fractions of nonerythrocytic spectrin extracts. Fractions of the nonerythrocytic spectrin extract from SEC (F) were coated onto ELISA plates, and binding of mClec9A-ecto (0.3 μg/ml) detected.
(H) Analysis of nonerythrocytic spectrin fractions by SDS-PAGE. Nonerythrocytic spectrin extract fractions from SEC (F) were analyzed by SDS-PAGE under reducing conditions and protein bands visualized by silver staining.
(I) Analysis of nonerythrocytic spectrin fractions by SDS-PAGE. Nonerythrocytic spectrin fractions 18–22 from SEC (F), corresponding to the Clec9A binding peak (G), were pooled, concentrated, and analyzed by SDS-PAGE under reducing conditions. Protein bands were visualized and bands F to H subjected to mass spectrometry analysis. See also Table S3.
See also Figure S3.

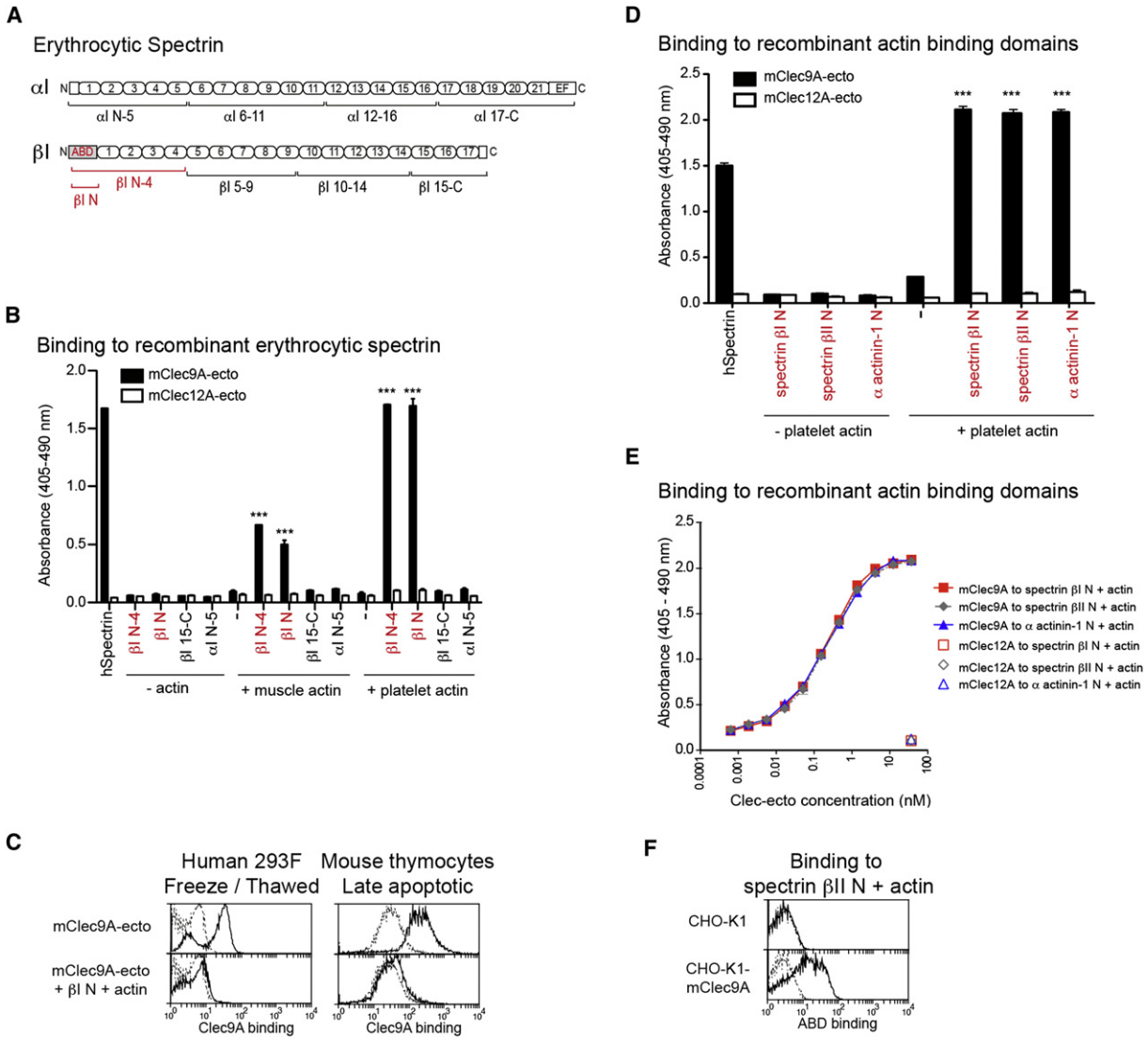

Figure 4. Clec9A Binds to a Complex of Actin with the Actin Binding Domain of Spectrin β1 and Other Cytoskeletal Proteins

(A) Schematic representation of the spectrin αI and βI proteins demonstrating the spectrin α1 repeats 1–21 and the C-terminal EF hand domains (EF), and the spectrin βI repeats 1–17 and the N-terminal actin binding domain (ABD). The regions encompassed by the recombinant spectrin fragments investigated are demonstrated below each chain.

(B) Clec9A binding to recombinant GST-tagged erythrocytic spectrin fragments in the presence or absence of actin. Recombinant spectrin was preassociated with either muscle or platelet actin (30°C) before coating onto ELISA plates and incubation with mClec9A-ecto (1 μg/ml) or the control protein mClec12A-ecto. Binding was detected with anti-FLAG-HRP. Cumulative data of four experiments are shown, demonstrating the mean ± standard errors of the mean (SEM). Clec9A-ecto binding to the βI N-4 + muscle actin was significantly greater than binding to βI N-4 alone ($p < 0.0001$) or to muscle actin alone ($p < 0.0005$). Similarly, Clec9A-ecto binding to βI N + muscle actin was significantly greater than binding to βI N alone or to muscle actin alone ($p < 0.0001$); Clec9A-ecto binding to βI N-4 + platelet actin and to βI N + platelet actin was significantly greater than binding to βI N or βI N-4 alone, respectively, or to platelet actin alone ($p < 0.0001$).

(C) Clec9A binding to dead cells is inhibited by preincubation of Clec9A with GST-tagged erythrocytic spectrin βI N plus actin. Preassociated spectrin βI N plus actin was incubated with mClec9A-ecto (0.5 hr, 21°C), before incubation with freeze-thawed 293F cells or with late apoptotic (PI^+) thymocytes. Binding of mClec9A-ecto (5 μg/ml; solid line) in the presence or absence of actin (50 μg/ml platelet actin for freeze-thawed 293F cells; 100 μg/ml muscle actin for apoptotic thymocytes) plus spectrin βI N (50–100 μg/ml) or the control Cire-ecto (dashed line) was detected with a FITC-conjugated FLAG mAb and flow cytometry.

(D) Clec9A binding to recombinant GST-tagged ABD of erythrocytic spectrin (spectrin βI N), nonerythrocytic spectrins (spectrin βII N), and α-actinin 1 (α-actinin 1 N) in the presence or absence of actin. Preassociated ABD ± platelet actin were coated onto ELISA plates and incubated with mClec9A-ecto (1 μg/ml) or mClec12A-ecto, and binding was detected with anti-FLAG-HRP. Cumulative data of three experiments are shown, demonstrating the mean ± SEM. Clec9A-ecto binding to the spectrin βI N + actin was significantly greater than binding to βI N alone ($p < 0.0001$) or to actin alone ($p < 0.0005$). Similarly, Clec9A-ecto binding to the spectrin βII N + actin was significantly greater than binding to βII N or to actin alone ($p < 0.0001$); Clec9A-ecto binding to α-actinin 1 N + actin was significantly greater than binding to α-actinin 1 N or to actin alone ($p < 0.0001$).

(E) Clec9A binding to recombinant GST-tagged spectrin βI N, spectrin βII N, and α-actinin 1 N in the presence or absence of actin. Preassociated ABD plus platelet actin were coated onto ELISA plates, and binding of mClec9A-ecto or mClec12A-ecto detected.

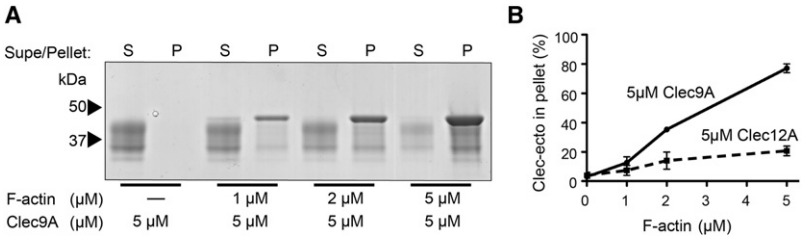

Figure 5. Clec9A Binds to Actin Filaments

Ectodomains of mClec9A (5 μM) were incubated with various concentrations of actin in the form of preformed muscle actin filaments, then centrifuged.

(A) An example of gel electrophoresis of the pellet (P) and supernatant (S) fractions.

(B) Quantitation of the proportion of mClec9A-ecto sedimenting with F-actin, compared to mClec12A-ecto as a nonspecific binding control. Data are mean ± SEM from three experiments.

murine sequence (NCD). The resulting protein, hCLEC9A-CTLD (S225D), maintained binding activity to dead cells as compared to the native hCLEC9A-CTLD (Figure S5A). Crystals diffracting to high resolution were obtained by including enterokinase in the crystallization drops to remove the extraneous N-terminal sequence including the FLAG tag.

The CLEC9A CTLD displayed the canonical fold of C-type lectin domains. A DALI search (Holm and Rosenström, 2010) revealed the CTLD of CLEC8A (LOX-1) (PDB: 1YPU) (Park et al., 2005) to have the strongest structural homology to the CLEC9A CTLD (Figure 6B). Crystals contained two copies of the CLEC9A CTLD within the asymmetric unit related by 2-fold symmetry (Figure 6A; Table S4). This dimer interface is unlike those previously characterized for CTLD domains (e.g., CLEC8A [Park et al., 2005], CD69 [Natarajan et al., 2000]). Because it is highly fenestrated and contains little buried surface area, this dimer is probably an artifact of crystallization. Furthermore, antibodies targeting a loop region within this dimer interface (position 185–211, shown in pink in Figures 6A and 6C) are biologically active and highly effective for targeting antigen to CLEC9A, indicating that this loop is exposed on cell surface CLEC9A. Full-length Clec9A exists as a disulphide-linked dimer on the cell surface (Figure S1B; Sancho et al., 2008), most probably mediated by cysteine residues in CLEC9A N-terminal stalk regions of the ecto-domain. Orientation of the CLEC9A CTLD in a CLEC8A style dimer revealed that the CLEC9A structure is compatible with such a dimer interface with only small refolding of a loop present at the top of the interface (166-KIKG-169) being required to remove backbone clashes (Figures 6B and 6C).

Crystal packing is mediated by burial of two exposed tryptophan residues (W131, W227; shown in blue, Figures 6A and 6C) into the edge of the crystallographic dimer groove of adjacent asymmetric units (Figure S5B). These tryptophans are conserved between the human and mouse. Although the tryptophans are unlikely to adopt these exposed conformations in solution, they are both located close to the human and murine glycosylation sites (Figure S5C). Within a monomer of the CLEC9A-CTLD, a Ca^{2+} ion was observed coordinated by E152, E156, E223, the peptide carbonyl of Q150, and two waters (Figure S5D). This site is analogous to a previously described Ca^{2+} binding site on CTLDs (site 4 [Zelensky and Gready, 2005]), where its role is to stabilize the structure of the protein rather than being directly involved in receptor-ligand interactions. Thermofluor assays confirmed that Ca^{2+} stabilizes, and EDTA destabilizes, the tertiary structure of hCLEC9A-CTLD (Figure S5E).

Regions of the Clec9A CTLD Involved in Ligand Recognition

In order to identify regions of CLEC9A involved in ligand recognition, constructs of the hCLEC9A ectodomain were prepared with a range of mutations. Like CLEC8A (Ohki et al., 2005), CLEC9A has a stretch of basic residues on or near the surface of the CLEC8A-style dimer (K166, K168, K215, K228; Figure S5F). Although CLEC9A mutant K228A did not express, mutants K166A, K168A, and K215A were expressed and exhibited binding to dead cells comparable to that of wild-type CLEC9A (Figure 7A). The most striking effects were obtained with the double mutant W131A, W227A (W131 and W227 shown in blue, Figure 6C). This mutant had comparable secondary structure to the original CLEC9A-CTLD based on circular dichroism analysis but showed functional differences in binding Clec9A ligands. This mutant did not bind freeze-thawed human nucleated cells, mouse erythrocyte saponin ghosts (Figures 7A and 7B), or human erythrocytic or nonerythrocytic spectrin (Figures 7C and 7D). Furthermore, it did not bind recombinant spectrin β1, spectrin βII, or α-actinin-1 ABD associated with actin (Figures 7E and 7F). All binding readouts were abrogated by the same mutation, so this further supports the hypothesis that actin in the filamentous form normally complexed with actin-binding proteins containing calponin homology-based ABD represent dead cell ligands recognized by Clec9A.

DISCUSSION

The response of the immune system to the danger posed by necrotic, late-apoptotic, or otherwise damaged cells depends on the initial recognition of particular DAMPs. Clec9A is a specialized DAMP recognition molecule, conserved from mouse to humans but restricted to the surface of the particular DC subsets that are especially efficient at processing material from dead cells. Our previous studies (Caminschi et al., 2008; Idoyaga et al., 2011; Lahoud et al., 2011) and that of the Reis e Sousa team (Sancho et al., 2008) have shown that targeting antigens to Clec9A on DCs in situ is an exceptionally efficient way of enhancing immune responses and so represents a promising

(F) Membrane-associated Clec9A binding to recombinant GST-tagged spectrin βII N and actin. CHO-K1 transfectant cells expressing full-length mClec9A, or parental CHO-K1 cells, were incubated with preassociated recombinant GST-tagged spectrin βII N and actin. Unbound spectrin-actin complexes were washed off and binding of spectrin-actin complexes was detected with a monoclonal mouse GST antibody followed by anti-mouse Ig-PE and flow cytometric analysis. See also Figure S4.

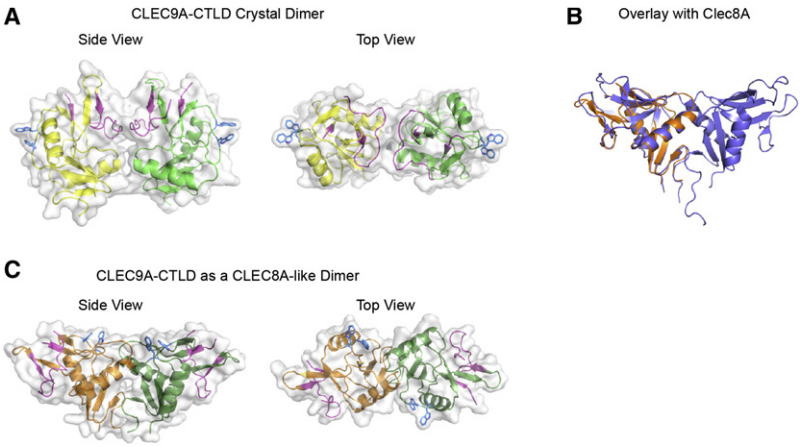

Figure 6. Crystal Structure of the hCLEC9A-C-type Lectin-like Domain

(A) Crystal structure of the hCLEC9A-CTLD dimer in the asymetric unit. This dimer is probably an artifact of crystallization. The conserved tryptophans (W131, W227) are presented in blue. The peptide region to which the CLEC9A Ab were raised (Caminschi et al., 2008) is shown in pink.

(B) Overlay of the hCLEC9A-CTLD monomer with the CLEC8A dimer. The CLEC9A CTLD monomer is displayed in orange; the CLEC8A dimer is displayed in blue.

(C) CLEC9A as a CLEC8A style dimer. Tryptophans (W131, W227) are shown in blue. The peptide region to which the CLEC9A Ab were raised is in pink.

See also Figure S5 and Table S4.

strategy for improving vaccines. The effectiveness of antibodies against Clec9A in targeting antigens to DCs and enhancing immune responses involves "hijacking" this uptake and processing system, so a single model vaccine antigen is handled with the same high efficiency as the multiple antigens from damaged cell material. Both the basic immunology of DAMP function and these practical implications for vaccine delivery prompted our investigation of the structure of Clec9A and the nature of its dead cell ligand.

In agreement with Sancho et al. (2009), we found that the Clec9A dead cell ligand is a normal cell component exposed when the cell membrane is ruptured. We find that the exposed cytoskeleton of the damaged cell provides the DAMPs recognized by Clec9A. Our results suggest that there is a limited window during which a damaged cell, such as a cell being destroyed by infection with a lytic virus or intracellular pathogen, would be detected by the Clec9A system. The early stages of apoptosis are not detected by Clec9A and it is likely that macrophages would eliminate most apoptotic cells at this stage. If any apoptotic cells persist, they would be recognized by Clec9A, along with cells undergoing necrotic death, soon after the membrane is ruptured but before digestion of the cytoskeletal structure by proteolytic enzymes. Because antigen delivery to Clec9A on DCs results in induction of potent humoral and cellular immunity, we postulate that uptake and processing of damaged or infected cell antigens associated with the cytoskeletal Clec9A ligand would similarly lead to activation of potent immune responses. The capacity of Clec9A also to bind the cytoskeleton of red cells may imply a role in early responses to malaria infection and other intracellular pathogens.

We have attempted to define in more precise molecular terms the cytoskeletal DAMPs recognized by Clec9A. In the case of damaged erythrocytes, we found that a multimeric complex of spectrin with actin binds to Clec9A with high affinity and represents a major ligand. Other C-type lectins do not bind this complex and the dissociated components of the complex do not bind to Clec9A. The minimal requirement for recognition by Clec9A appeared to be a form of actin complexed with the calponin homology ABDs of cytoskeletal molecules, including spectrin β chains and α-actinins. In the case of nucleated cells where there are several molecules containing such domains, additional structures of this form would be exposed upon cell damage. This posed the question of whether it was the complex structure itself that was recognized, or some conformational change in the ABDs or in actin subsequent to the interaction. The finding that Clec9A binds directly to filaments of actin suggests that the latter is the case. The ABDs may either catalyze the formation of actin filaments or may help maintain actin in this particular filamentous structure. Because cofilin bound to actin did not bind Clec9A, and because cofilin remodels the structure of actin filaments (Galkin et al., 2011), only particular forms of filamentous actin appear to bind Clec9A. Our immunofluorescence results indicating that Clec9A binds to certain actin filaments rather than all the actin in the cell supports this model. Although F-actin may be the basic structure recognized, actin filaments in a cell would always be associated with a number of molecules with the appropriate ABDs, and Clec9A would bind to this entire cytoskeletal complex when it is exposed by cell damage.

We have performed structural studies on the other half of this recognition system, the CLEC9A-CTLD itself. These suggest that CLEC9A could form a dimer with structural homology to CLEC8A; confirmation of this will require crystallization of the CLEC9A ectodomain including the stalk region. The structure of the CTLD has also revealed other features related to CLEC9A functions. A Ca^{2+} ion is coordinated within the structure, as observed in other CTLDs (site 4 as described by Zelensky and Gready, 2005). We find no evidence that calcium is directly involved in ligand interaction, consistent with previous reports of CTLDs with a site 4 Ca^{2+} ion, and unlike CTLDs with a site 2 Ca^{2+} that coordinates at a ligand-receptor interface (Zelensky and Gready, 2005). Rather, it plays a structural role with a stabilizing effect, again consistent with the observed role of this Ca^{2+} site in other CTLDs. Two tryptophans, conserved between the human and mouse CLEC9A and located in a potentially exposed region, are crucial to DAMP recognition by CLEC9A. Mutation at these sites ablates binding to dead nucleated cells, to erythrocyte ghosts, and to actin complexed with spectrin-ABD and α-actinin-ABD. The finding that the mutation affects all three supports the case that actin filaments in the form normally complexed with particular cytoskeletal ABDs is the ligand recognized on damaged cells. It is notable that our targeting Clec9A monoclonal antibodies that enhance immune responses were directed against peptides well outside this region. Antibodies or other

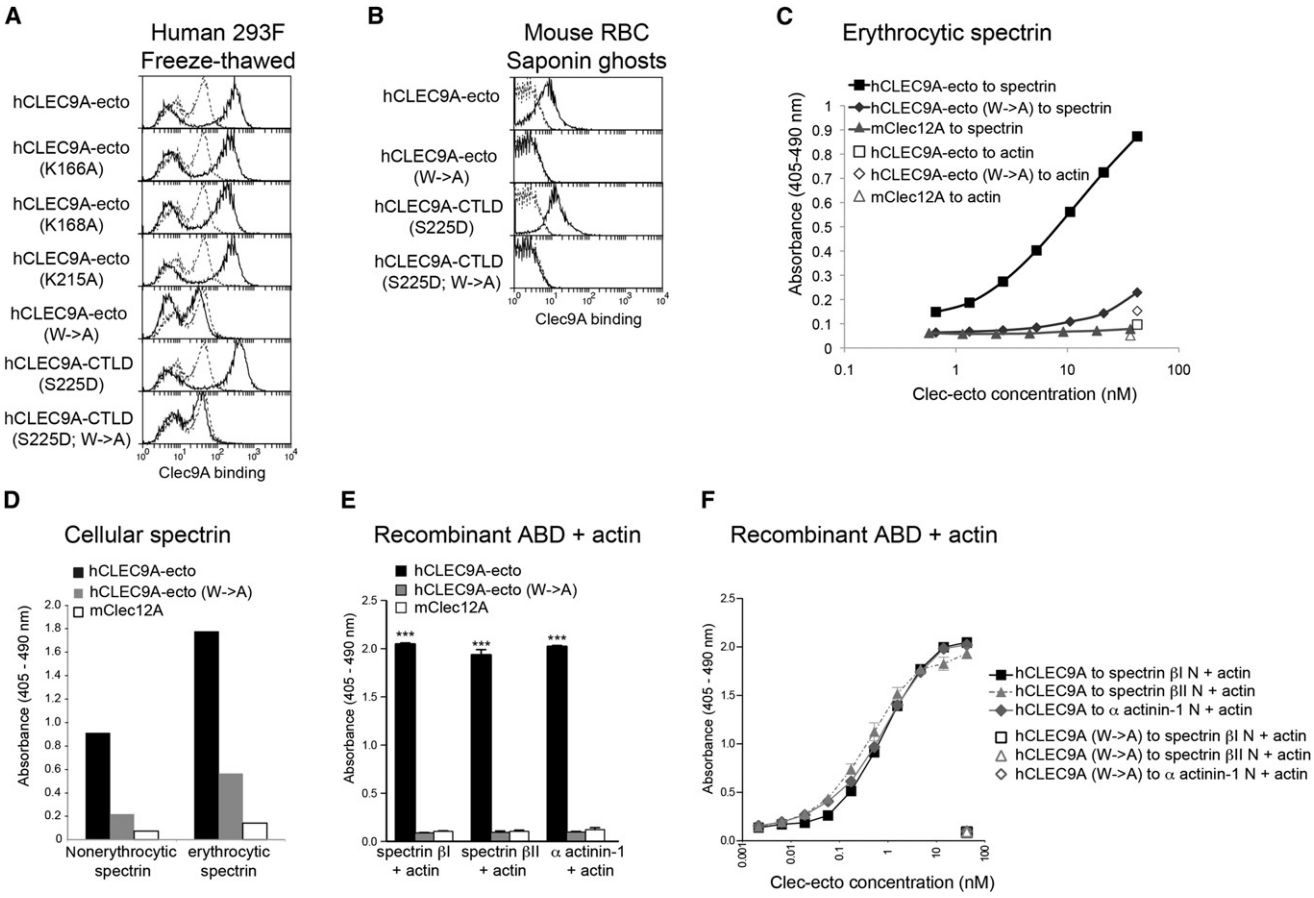

Figure 7. Structural Requirements for Clec9A Binding to Ligands

(A) CLEC9A binding to dead cells requires Trp-mediated interactions. Wild-type and mutated hCLEC9A (K166A, K168A, K215A, and W131A and W227A shown as W→A) ectodomains and CTLD were generated and binding examined to freeze-thawed human 293F cells (solid line). Binding of the control Clec12A is indicated (dashed line). Clec binding was detected with a FITC-conjugated FLAG mAb and flow cytometry.

(B) CLEC9A binding to RBC ghosts requires Trp-mediated interactions. Wild-type and mutated hCLEC9A (W131A and W227A shown as W→A) ectodomains and CTLD were examined for binding to saponin-permeabilized mouse RBC ghosts (solid line). Binding of the control Clec12A is indicated (dashed line). Clec binding was detected with a FITC-conjugated FLAG mAb and flow cytometry.

(C) CLEC9A binding to human erythroid spectrin requires Trp-mediated interactions. Erythroid spectrin (Sigma) was coated onto plates, and binding of wild-type and mutated CLEC9A-ecto and controls were detected by ELISA with FLAG mAb HRP.

(D) Clec9A binding to spectrin requires Trp-mediated interactions. Erythroid spectrin (Sigma) and nonerythroid spectrin isolated from nucleated 293F cells were coated onto plates. Binding of wild-type and mutated CLEC9A-ecto and controls (1 μg/ml) was detected by ELISA.

(E) Clec9A binding to ABD-actin complexes requires Trp-mediated interactions. Preassociated complexes of the ABD of erythrocytic spectrin (spectrin βI N), nonerythrocytic spectrins (spectrin βII N), and α-actinin 1 (α-actinin 1 N) with platelet actin were coated onto plates. Binding of wild-type and mutated CLEC9A-ecto and controls (1 μg/ml) was detected by ELISA by FLAG mAb HRP. Cumulative data of three experiments are shown, demonstrating the mean ± SEM. Binding of the wild-type hCLEC9A-ecto binding to the spectrin βI N + actin, spectrin βII N + actin, or α-actinin 1 N + actin was significantly greater than binding of the mutated hCLEC9A-ecto (W→A) (***$p < 0.0001$) or the binding of the control Clec12A-ecto (***$p < 0.0001$) to the ABD-actin complexes.

(F) Clec9A binding to ABD-actin complexes requires Trp-mediated interactions. Spectrin βI N, spectrin βII N, and α-actinin 1 N were associated with platelet actin and coated onto plates. Binding of wild-type and mutated CLEC9A-ecto and controls was detected by ELISA with FLAG mAb HRP. Cumulative data of three experiments are shown, demonstrating the mean ± SEM.

antagonists of this ligand-binding region of Clec9A may be powerful inhibitors of the immune responses initiated by the Clec9A-bearing DC subtypes.

The recognition of actin filaments of damaged cells by Clec9A on DC subtypes has the potential to play an important role both in enhancing immunity to intracellular infections and in exacerbating autoimmune diseases, such as systemic lupus erythematosus. Harnessing the knowledge revealed in this study of the Clec9A structural requirements for actin filament recognition will facilitate the design of agonistic and antagonistic molecules that may lay the basis of therapeutic strategies for human disease.

EXPERIMENTAL PROCEDURES

Isolation of Primary Cells

Female C57BL/6J Wehi mice, 8–12 weeks of age, were bred under specific-pathogen-free conditions at The Walter and Eliza Hall Institute (WEHI). Animals

were handled according to the guidelines of the National Health and Medical Research Council of Australia. Experimental procedures for isolation of mouse and human primary cells were approved by the Animal Ethics Committee and Human Research Ethics Committee, WEHI.

Generation of Clec Ectodomains

cDNA fragments encoding all or part of Clec9A ectotodomains were amplified from the original *Clec9A* cDNA sequence (Caminschi et al., 2008) or were synthesized with the required mutations and subcloned into either a pEF-Bos or a pcDNA3.1$^+$ expression vector modified to encode a FLAG tag and a biotinylation consensus sequence (Brown et al., 1998). Clec ectodomains were expressed in mammalian cells and purified with anti-FLAG resin and size-exclusion chromatography (SEC) (Supplemental Experimental Procedures). FLAG-tagged ectodomains of two mouse C-type lectin molecules including Cire (mouse DC-Sign) (Caminschi et al., 2001) and Clec12A (Lahoud et al., 2009; Pyz et al., 2008) were generated as controls. Recombinant soluble Clec ectodomains were either enzymatically biotinylated and detected with streptavidin-PE (SA-PE) or detected with anti-FLAG reagents.

Crystallization and Structure Determination

Crystals of purified, glycosylation-null, human CLEC9A-CTLD (S225D) were grown in hanging drops at 4°C (reservoir solution; 30% PEG8000, 0.2 M $MgCl_2$, 0.1 M Tris [pH 8.0], drop supplemented with a 1:50 molar ratio of enterokinase). Crystals were equilibrated in cryo-protectant consisting of reservoir solution supplemented with 15% (v/v) ethylene glycol and then flash-frozen in liquid N2. X-ray data were collected at the Australian Synchrotron on beamline PX2 at 100 K. The data were processed with XDS (Kabsch, 2010). The structure was solved by molecular replacement with PHASER (McCoy et al., 2007) and a Chainsaw (Stein, 2008) modified model of CD69 as the search model (PDB: 1FM5) (Natarajan et al., 2000). Several rounds of building were performed in COOT (Emsley and Cowtan, 2004) and refinement in PHENIX (Adams et al., 2010) incorporating simulated annealing, TLS, individual site refinement, and individual ADP refinement. The final refinement statistics are given in Table S4.

Cytoskeletal Proteins

Cellular spectrin complexes were isolated as in Gratzer (1982) and Ungewickell and Gratzer (1978), then purified by SEC (Supplemental Experimental Procedures). Spectrins were reassociated with actin by concentrating dissociated spectrin in the presence of either bovine muscle actin or a control protein BSA, followed by incubation for 2.5 hr at 30°C and further purification by SEC.

Recombinant GST-tagged cofilin-1 (Wong et al., 2011) and GST-tagged fragments of erythrocytic spectrin (spectrin βI) (Pei et al., 2005), nonerythrocytic spectrin (spectrin βII), and α-actinin I were expressed and purified with Glutathione-Sepharose 4B resin and SEC (Supplemental Experimental Procedures). Reassociation of ABD with actin was performed by incubating GST-tagged spectrin and actinin proteins with bovine muscle actin (Sigma) or platelet actin (>99% purity, Cytoskeleton) for 2 hr at 4°C.

ELISA

ELISA plates were coated with cellular or recombinant spectrin complexes and controls, blocked, then incubated with FLAG-tagged Clec9A ectodomain fragments or controls (mClec12A-ecto, mCire-ecto). Binding was detected with anti-FLAG HRP (Supplemental Experimental Procedures). Statistical analysis of ELISA data was performed by an unpaired two-tailed t test on log-transformed data. The significance of difference is indicated as ***$p < 0.0001$. Analysis was performed in Prism (GraphPad Software).

Sedimentation Binding Assay

Full details are in Wong et al. (2011). G-actin was purified from a rabbit muscle actin preparation (Cytoskeleton) by SEC, then transformed into F-actin. Various concentrations of the actin filaments were mixed with the ectodomains of mClec9A or mClec12A for 30 min at room temperature and then centrifuged at 100,000 × g for 1 hr. Supernatant and pellet fractions were analyzed by SDS-PAGE.

ACCESSION NUMBERS

The atomic coordinates and structure factors for CLEC9A (PDB ID code 3VPP) have been deposited in the Protein Data Bank, Research Collaboratory for Structural Bioinformatics, Rutgers University (http://www.rcsb.org).

SUPPLEMENTAL INFORMATION

Supplemental Information includes Supplemental Experimental Procedures, five figures, and four tables and can be found with this article online at doi:10.1016/j.immuni.2012.03.009.

ACKNOWLEDGMENTS

We thank A. Cowman and R. Simpson for critical discussions and L. Zhang for his assistance with CD measurements. We thank L. Connolly, H. Patsiouras, and T. Nebl for MS sequencing analysis. Crystallization trials were performed at the Bio21 Collaborative Crystallisation Centre, Australia. Diffraction data were collected at the Australian Synchrotron and we thank staff for their assistance. This work was supported by the National Health and Medical Research Council of Australia (NHMRC) program grants 454465 (K.S.), 461219 (N.A.N., J.-G.Z.), and 461221 (D.C.S.H.), project grants 575546 (K.S., M.H.L., I.C.) and 1009145 (L.O.R.), Human Frontier Science Program (J.B.), Australian Research Council Future Fellowships (P.E.C., J.B.), NHMRC fellowships (K.S., P.M.C., N.A.N., D.C.S.H.), NHMRC Career Development Fellowship (J.D.M.), Australian Cancer Research Foundation (P.M.C., D.C.S.H.), Leukemia & Lymphoma Society Grant SCOR 7413 (D.C.S.H., L.O.R.) and Fellowship (E.C.J.), Melbourne University International Research Scholarship (M.F.v.D.), and Cancer Council Victoria Postdoctoral Research Fellowship (M.F.v.D.). This work was made possible through Victorian State Government Operational Infrastructure Support and Australian Government NHMRC IRIIS.

Received: September 12, 2011
Revised: February 8, 2012
Accepted: March 18, 2012
Published online: April 5, 2012

REFERENCES

Adams, P.D., Afonine, P.V., Bunkóczi, G., Chen, V.B., Davis, I.W., Echols, N., Headd, J.J., Hung, L.W., Kapral, G.J., Grosse-Kunstleve, R.W., et al. (2010). PHENIX: a comprehensive Python-based system for macromolecular structure solution. Acta Crystallogr. D Biol. Crystallogr. *66*, 213–221.

An, X., Guo, X., Yang, Y., Gratzer, W.B., Baines, A.J., and Mohandas, N. (2011). Inter-subunit interactions in erythroid and non-erythroid spectrins. Biochim. Biophys. Acta *1814*, 420–427.

Baines, A.J. (2010). The spectrin-ankyrin-4.1-adducin membrane skeleton: adapting eukaryotic cells to the demands of animal life. Protoplasma *244*, 99–131.

Banchereau, J., Briere, F., Caux, C., Davoust, J., Lebecque, S., Liu, Y.J., Pulendran, B., and Palucka, K. (2000). Immunobiology of dendritic cells. Annu. Rev. Immunol. *18*, 767–811.

Bergeron, S.E., Zhu, M., Thiem, S.M., Friderici, K.H., and Rubenstein, P.A. (2010). Ion-dependent polymerization differences between mammalian beta- and gamma-nonmuscle actin isoforms. J. Biol. Chem. *285*, 16087–16095.

Brown, M.H., Boles, K., van der Merwe, P.A., Kumar, V., Mathew, P.A., and Barclay, A.N. (1998). 2B4, the natural killer and T cell immunoglobulin superfamily surface protein, is a ligand for CD48. J. Exp. Med. *188*, 2083–2090.

Caminschi, I., Lucas, K.M., O'Keeffe, M.A., Hochrein, H., Laâbi, Y., Brodnicki, T.C., Lew, A.M., Shortman, K., and Wright, M.D. (2001). Molecular cloning of a C-type lectin superfamily protein differentially expressed by CD8alpha(-) splenic dendritic cells. Mol. Immunol. *38*, 365–373.

Caminschi, I., Proietto, A.I., Ahmet, F., Kitsoulis, S., Shin Teh, J., Lo, J.C., Rizzitelli, A., Wu, L., Vremec, D., van Dommelen, S.L., et al. (2008). The dendritic cell subtype-restricted C-type lectin Clec9A is a target for vaccine enhancement. Blood *112*, 3264–3273.

Emsley, P., and Cowtan, K. (2004). Coot: model-building tools for molecular graphics. Acta Crystallogr. D Biol. Crystallogr. *60*, 2126–2132.

Galkin, V.E., Orlova, A., Kudryashov, D.S., Solodukhin, A., Reisler, E., Schröder, G.F., and Egelman, E.H. (2011). Remodeling of actin filaments by ADF/cofilin proteins. Proc. Natl. Acad. Sci. USA *108*, 20568–20572.

Gratzer, W.B. (1982). Preparation of spectrin. Methods Enzymol. *85*, *Pt B*, 475–480.

Holm, L., and Rosenström, P. (2010). Dali server: conservation mapping in 3D. Nucleic Acids Res. *38* (Web Server issue), W545–W549.

Huysamen, C., Willment, J.A., Dennehy, K.M., and Brown, G.D. (2008). CLEC9A is a novel activation C-type lectin-like receptor expressed on BDCA3+ dendritic cells and a subset of monocytes. J. Biol. Chem. *283*, 16693–16701.

Idoyaga, J., Lubkin, A., Fiorese, C., Lahoud, M.H., Caminschi, I., Huang, Y., Rodriguez, A., Clausen, B.E., Park, C.G., Trumpfheller, C., and Steinman, R.M. (2011). Comparable T helper 1 (Th1) and CD8 T-cell immunity by targeting HIV gag p24 to CD8 dendritic cells within antibodies to Langerin, DEC205, and Clec9A. Proc. Natl. Acad. Sci. USA *108*, 2384–2389.

Kabsch, W. (2010). Xds. Acta Crystallogr. D Biol. Crystallogr. *66*, 125–132.

Korenbaum, E., and Rivero, F. (2002). Calponin homology domains at a glance. J. Cell Sci. *115*, 3543–3545.

Lahoud, M.H., Proietto, A.I., Ahmet, F., Kitsoulis, S., Eidsmo, L., Wu, L., Sathe, P., Pietersz, S., Chang, H.W., Walker, I.D., et al. (2009). The C-type lectin Clec12A present on mouse and human dendritic cells can serve as a target for antigen delivery and enhancement of antibody responses. J. Immunol. *182*, 7587–7594.

Lahoud, M.H., Ahmet, F., Kitsoulis, S., Wan, S.S., Vremec, D., Lee, C.N., Phipson, B., Shi, W., Smyth, G.K., Lew, A.M., et al. (2011). Targeting antigen to mouse dendritic cells via Clec9A induces potent CD4 T cell responses biased toward a follicular helper phenotype. J. Immunol. *187*, 842–850.

McCoy, A.J., Grosse-Kunstleve, R.W., Adams, P.D., Winn, M.D., Storoni, L.C., and Read, R.J. (2007). Phaser crystallographic software. J. Appl. Cryst. *40*, 658–674.

Natarajan, K., Sawicki, M.W., Margulies, D.H., and Mariuzza, R.A. (2000). Crystal structure of human CD69: a C-type lectin-like activation marker of hematopoietic cells. Biochemistry *39*, 14779–14786.

Ohki, I., Ishigaki, T., Oyama, T., Matsunaga, S., Xie, Q., Ohnishi-Kameyama, M., Murata, T., Tsuchiya, D., Machida, S., Morikawa, K., and Tate, S. (2005). Crystal structure of human lectin-like, oxidized low-density lipoprotein receptor 1 ligand binding domain and its ligand recognition mode to OxLDL. Structure *13*, 905–917.

Park, H., Adsit, F.G., and Boyington, J.C. (2005). The 1.4 angstrom crystal structure of the human oxidized low density lipoprotein receptor lox-1. J. Biol. Chem. *280*, 13593–13599.

Pei, X., An, X., Guo, X., Tarnawski, M., Coppel, R., and Mohandas, N. (2005). Structural and functional studies of interaction between *Plasmodium falciparum* knob-associated histidine-rich protein (KAHRP) and erythrocyte spectrin. J. Biol. Chem. *280*, 31166–31171.

Pyz, E., Huysamen, C., Marshall, A.S., Gordon, S., Taylor, P.R., and Brown, G.D. (2008). Characterisation of murine MICL (CLEC12A) and evidence for an endogenous ligand. Eur. J. Immunol. *38*, 1157–1163.

Rotter, B., Kroviarski, Y., Nicolas, G., Dhermy, D., and Lecomte, M.C. (2004). AlphaII-spectrin is an in vitro target for caspase-2, and its cleavage is regulated by calmodulin binding. Biochem. J. *378*, 161–168.

Sancho, D., Mourão-Sá, D., Joffre, O.P., Schulz, O., Rogers, N.C., Pennington, D.J., Carlyle, J.R., and Reis e Sousa, C. (2008). Tumor therapy in mice via antigen targeting to a novel, DC-restricted C-type lectin. J. Clin. Invest. *118*, 2098–2110.

Sancho, D., Joffre, O.P., Keller, A.M., Rogers, N.C., Martínez, D., Hernanz-Falcón, P., Rosewell, I., and Reis e Sousa, C. (2009). Identification of a dendritic cell receptor that couples sensing of necrosis to immunity. Nature *458*, 899–903.

Shortman, K., and Heath, W.R. (2010). The CD8+ dendritic cell subset. Immunol. Rev. *234*, 18–31.

Stein, N. (2008). CHAINSAW: a program for mutating pdb files used as templates in molecular replacement. J. Appl. Cryst. *41*, 641–643.

Steinman, R.M., Hawiger, D., and Nussenzweig, M.C. (2003). Tolerogenic dendritic cells. Annu. Rev. Immunol. *21*, 685–711.

Ungewickell, E., and Gratzer, W. (1978). Self-association of human spectrin. A thermodynamic and kinetic study. Eur. J. Biochem. *88*, 379–385.

Uribe, R., and Jay, D. (2009). A review of actin binding proteins: new perspectives. Mol. Biol. Rep. *36*, 121–125.

van Delft, M.F., Wei, A.H., Mason, K.D., Vandenberg, C.J., Chen, L., Czabotar, P.E., Willis, S.N., Scott, C.L., Day, C.L., Cory, S., et al. (2006). The BH3 mimetic ABT-737 targets selective Bcl-2 proteins and efficiently induces apoptosis via Bak/Bax if Mcl-1 is neutralized. Cancer Cell *10*, 389–399.

Villadangos, J.A., and Shortman, K. (2010). Found in translation: the human equivalent of mouse CD8+ dendritic cells. J. Exp. Med. *207*, 1131–1134.

Wong, W., Skau, C.T., Marapana, D.S., Hanssen, E., Taylor, N.L., Riglar, D.T., Zuccala, E.S., Angrisano, F., Lewis, H., Catimel, B., et al. (2011). Minimal requirements for actin filament disassembly revealed by structural analysis of malaria parasite actin-depolymerizing factor 1. Proc. Natl. Acad. Sci. USA *108*, 9869–9874.

Zelensky, A.N., and Gready, J.E. (2005). The C-type lectin-like domain superfamily. FEBS J. *272*, 6179–6217.